An ab Initio Study of Hydrogen Atom Abstractions from Substituted Methanes by Substituted Methyl Radicals

Gary L. Fox and H. B. Schlegel*

Department of Chemistry, Wayne State University, Detroit, Michigan 48202 *(Received: July 16, 1991)*

The reactions $CH_3X + {}^{\bullet}CH_2Y \rightarrow {}^{\bullet}CH_2X + CH_3Y$ (X, Y = H, F, Cl, OH, NH_2, CN) have been studied using ab initio molecular orbital theory at the UHF/3-21G and UHF/6-31G** levels. The Marcus relation can be used to predict the barrier heights of the cross reactions based on the information from the identity reactions and the changes in energy for the cross reactions. This method predicts the barrier heights accurately with two exceptions (X = CN and Y = NH_2 or OH); the average absolute error is 0.98 kcal/mol when compared to the ab initio barrier heights. Charge-transfer states have been found to play a significant role in the reactions where X = CN and Y = NH_2 or OH and a minor role in a few other reactions.

Introduction

Theories for predicting reaction rates and barriers are extremely useful tools of both experimental and theoretical chemists.[1] These theories can be used as predictive tools when experimental results are lacking or as supporting evidence for the mechanisms of reactions. One such approach is Marcus theory[2] which was developed to describe electron-transfer processes and has been expanded to include proton transfer[3] and methyl group transfer[4] reactions. Marcus theory expresses the barrier for the cross reactions ($\Delta E^{\ddagger}_{XY}$) in terms of an intrinsic barrier, $\Delta E^{\ddagger}_{I}$ and the change in energy of the reaction, ΔE_{rxn}.

$$\Delta E^{\ddagger}_{XY} = {}^1/_2\Delta E_{rxn} + \Delta E^{\ddagger}_{I} + \frac{(\Delta E_{rxn})^2}{16\Delta E^{\ddagger}_{I}} \qquad (1)$$

The intrinsic barrier, $\Delta E^{\ddagger}_{I}$, is often estimated by the arithmetic average of the symmetric reaction barriers ($\Delta E^{\ddagger}_{I} = {}^1/_2[\Delta E^{\ddagger}_{XX} + \Delta E^{\ddagger}_{YY}]$). Thus, if intrinsic barriers are available for a few symmetric reactions, the barrier heights for a wide variety of reactions can be predicted from the heats of reaction. If Marcus theory can reproduce the barrier heights for hydrogen-abstraction reactions, it will help unify and simplify the treatment of barrier heights and substituent effects for this class of reactions. It may also be possible to extend Marcus theory to other classes of abstraction reactions.

It is noteworthy to point out that all of the information needed to predict the barrier heights via Marcus theory can be calculated easily. The geometries and total energies of the reactants and products are obtained by simple optimizations to minima on the potential energy surfaces; the symmetric transition states (X = Y) needed to compute the intrinsic barriers can be located by minimization within the symmetry constraints of the transition states. The energy differences, ΔE_{rxn}, $\Delta E^{\ddagger}_{XX}$, and $\Delta E^{\ddagger}_{YY}$ can then be calculated directly from these total energies.

In the present study we have tested the barrier heights predicted via Marcus theory against the ab initio calculated barriers for the following radical abstraction reactions:

$$CH_3X + {}^{\bullet}CH_2Y \rightarrow {}^{\bullet}CH_2X + CH_3Y$$
$$(X, Y = H, F, Cl, OH, NH_2, CN) \qquad (2)$$

It is our immediate goal to test the utility of this methodology for this class of reactions and not to reproduce the experimental barriers of reaction. Calculations accurate enough to compare with experimental rates would require a larger basis set, the inclusion of electron correlation corrections, and a proper treatment of the reaction dynamics including tunneling, which is known to be significant for these heavy-light-heavy reactions.[5]

Method

Many of the geometries of the reactants and products were obtained from the Quantum Chemistry Archive,[6] and the remaining geometries of the reactants, products, and transition states were optimized using analytic gradient techniques[7] at the HF/3-21G and HF/6-31G** levels of theory (UHF for open shell and RHF for closed shell molecules) using the GAUSSIAN 90 series of programs.[8] The stationary points on the potential energy surfaces were characterized by the analytic calculation of vibrational frequencies.[9] All of the reactants and products have only real frequencies; each transition state has exactly one imaginary frequency corresponding to the breaking of the reactant carbon-

(1) See Murdoch, J. R. *J. Am. Chem. Soc.* **1983**, *105*, 2159 for an overview of empirical theories for predicting reaction barrier heights.

(2) (a) Marcus, R. A. *J. Chem. Phys.* **1956**, *24*, 966. (b) Marcus, R. A. *J. Chem. Phys.* **1956**, *24*, 979. (c) Marcus, R. A. *J. Chem. Phys.* **1957**, *26*, 867. (d) Marcus, R. A. *J. Chem. Phys.* **1957**, *26*, 872. (e) Marcus, R. A. *Can. J. Chem.* **1959**, *37*, 155. (f) Marcus, R. A. *Discuss. Faraday Soc.* **1960**, *29*, 21. (g) Marcus, R. A. *J. Phys. Chem.* **1963**, *67*, 853. (h) Marcus, R. A. *Annu. Rev. Phys. Chem.* **1964**, *15*, 155. (i) Marcus, R. A. *J. Chem. Phys.* **1965**, *43*, 679. (j) Marcus, R. A. *Exch. React. Proc. Symp.* **1965**, 1. (k) For an overview and history of Marcus theory and applications see the Rudolph A. Marcus Commemorative issue *J. Phys. Chem.* **1986**, *90*(16) and references therein.

(3) (a) Marcus, R. A. *J. Phys. Chem.* **1966**, *72*, 891. (b) Murdoch, J. R. *J. Am. Chem. Soc.* **1972**, *94*, 4410. (c) Murdoch, J. R.; Bryson, J. A.; McMillen, D. F.; Brauman, J. I. *J. Am. Chem. Soc.* **1982**, *104*, 600. (d) Murdoch, J. R.; Magnoli, D. E. *J. Am. Chem. Soc.* **1982**, *104*, 3792. (e) Magnoli, D. E.; Murdoch, J. R. *J. Am. Chem. Soc.* **1981**, *103*, 7465.

(4) (a) Albery, W. J. *Pure Appl. Chem.* **1979**, *51*, 949. (b) Kreevoy, W. J.; Kreevoy, M. M. *Adv. Phys. Org. Chem.* **1978**, *16*, 87. (c) Albery, W. *Ann. Rev. Phys. Chem.* **1980**, *31*, 277. (d) Lewis, E. S. *J. Phys. Chem.* **1986**, *90*, 3756. (e) Lewis, E. S. *Bull. Soc. Chim. Fr.* **1988**, No. 2, 259. (f) Lewis, E. S.; Hu, D. D. *J. Am. Chem. Soc.* **1984**, *106*, 3292. (g) Lewis, E. S.; Douglas, T. A.; McLaughlin, M. L. *Isr. J. Chem.* **1985**, *26*, 331. (h) Lewis, E. S.; Douglas, T. A.; McLaughlin, M. L. In *Nucleophilicity*; Harris, J. M., McManus, S. P., Eds.; ACS Advances in Chemistry Series No. 215; American Chemical Society: Washington, DC, 1987. (i) Kreevoy, M. M.; Ostovic, D.; Lee, I. S. H.; Binder, D. A.; King, G. W. *J. Am. Chem. Soc.* **1988**, *110*, 524. (j) Pellerite, M. J.; Brauman, J. I. *J. Am. Chem. Soc.* **1980**, *102*, 5993. (k) Dodd, J. A.; Brauman, J. I. *J. Am. Chem. Soc.* **1984**, *106*, 5356. (l) Dodd, J. A.; Brauman, J. I. *J. Phys. Chem.* **1986**, *90*, 3559. (m) Pellerite, M. J; Brauman, J. I. *J. Am. Chem. Soc.* **1983**, *105*, 2672. (n) Wolfe, S.; Mitchell, D. J.; Schlegel, H. B. *J. Am. Chem. Soc.* **1981**, *103*, 7692. (o) Wolfe, S.; Mitchell, D. J.; Schlegel, H. B. *J. Am. Chem. Soc.* **1981**, *103*, 7694.

(5) (a) Truhlar, D. G.; Gordon, M. S. *Science* **1990**, *249*, 491. (b) Truhlar, D. G.; Garret, B. C. *Acc. Chem. Res.* **1980**, *13*, 440.

(6) Whiteside, R. A.; Frisch, M. J.; Pople, J. A. *The Carnegie-Mellon Quantum Chemistry Archive*, 3rd ed.; Carnegie-Mellon University: Pittsburgh, PA, 1983, and associated computer data base.

(7) Schlegel, H. B. *J. Comput. Chem.* **1982**, *3*, 214.

(8) Frisch, M. J.; Head-Gordon, M.; Trucks, G. W.; Foresman, J. B.; Schlegel, H. B.; Raghavachari, K.; Robb, M.; Binkley, J. S.; Gonzalez, C.; Defrees, D. J.; Fox, D. J.; Whiteside, R. A.; Seeger, R.; Melius, C. F.; Baker, J.; Martin, R. L.; Kahn, L. R.; Stewart, J. J. P.; Topiol, S.; Pople, J. A. *Gaussian 90, Revision H*; Gaussian, Inc.: Pittsburgh, PA, 1990.

(9) Pople, J. A.; Schlegel, H. B.; Krishnan, R.; DeFrees, D. J.; Binkley, J. S.; Frisch, M. J.; Whiteside, R. A.; Hout, R. F.; Hehre, W. J. *Int. J. Quant. Chem. Symp.* **1981**, *15*, 269.

0022-3654/92/2096-298$03.00/0

TABLE I: Total Energies, S^2 Values, and Zero Point Energies for the Transition States

	UHF/3-21G			UHF/6-31G**		
X, Y	E(au)	S^2	ZPE (kcal/mol)	E(au)	S^2	ZPE (kcal/mol)
H, H	-79.276 139	0.793	49.97	-79.718 777 5	0.791	49.10
F, F	-275.889 676	0.793	41.84	-277.398 360 0	0.792	41.58
Cl, Cl	-992.701 862	0.793	39.61	-997.515 603 8	0.791	39.58
OH, OH	-228.123 005	0.793	56.67	-229.412 993 2	0.792	57.27
NH_2, NH_2	-188.699 352	0.792	74.38	-189.771 196 7	0.793	74.95
CN, CN	-261.718 100	0.972	50.37	-263.188 473 3	0.901	49.38
Cl, F	-634.296 337	0.793	40.77	-637.457 312 4	0.792	40.63
CN, NH_2[a]	-225.214 264	0.868	62.54	-226.484 978 6	0.837	62.36
CN, NH_2[b]	-225.214 264	0.868	62.54	-226.484 978 3	0.837	62.35
F, H	-177.583 005	0.793	45.92	-178.558 669 6	0.791	45.40
NH_2, OH	-208.415 410	0.792	66.16	-209.592 231 2	0.792	66.14
Cl, H	-535.989 995	0.792	44.85	-538.617 675 5	0.791	44.40
OH, Cl	-610.413 846	0.792	58.65	-613.465 241 4	0.791	48.39
CN, OH[a]	-244.926 482	0.862	54.21	-246.308 366 6	0.833	54.27
CN, OH[b]	-244.922 851	0.871	53.50	-246.303 527 2	0.837	53.24
OH, F	-252.007 079	0.793	49.22	-253.406 100 9	0.792	49.43
NH_2, Cl	-590.704 158	0.791	57.00	-593.645 403 8	0.791	57.31
OH, H	-153.698 894	0.793	53.29	-154.565 509 6	0.791	53.23
NH_2, F	-232.298 439	0.792	58.65	-233.585 326 0	0.792	58.26
CN, Cl	-627.209 610	0.868	45.02	-630.352 431 8	0.839	44.53
CN, F	-268.804 665	0.872	46.20	-270.294 934 8	0.838	45.65
NH_2, H	-133.988 297	0.792	62.22	-134.745 493 9	0.792	62.07
CN, H	-170.498 505	0.864	50.29	-171.455 537 1	0.833	49.37

[a] C_1 symmetry. [b] C_s symmetry.

TABLE II: Partial Summary of the Structures of the UHF/6-31G Transition States[a,b]**

X, Y	r_1	r_2	r_3	r_4	r_5	r_6	a	b	c	d	e	Ω_1	Ω_2
H, H	1.3560		1.0804				180.00	105.56				120.00	
F, F	1.3581		1.3512		1.0800		180.00	106.88		106.54		118.91	
Cl, Cl	1.3456		1.7577		1.0766		180.00	107.53		105.85		119.10	
OH, OH	1.3501		1.3854		1.0843		180.00	104.29		104.86		120.55	
NH_2, NH_2	1.3813		1.4297		1.0828		180.00	113.32		104.34		121.80	
CN, CN	1.3590		1.4393		1.0785		180.00	106.88		103.30		120.60	
Cl, F	1.3570	1.3453	1.7617	1.3485	1.0767	1.0798	183.58	107.43	106.76	106.23	106.24	118.99	118.91
CN, NH_2[c]	1.4087	1.3375	1.4379	1.4140	1.0788	1.0812	178.21	107.59	113.52	103.84	102.79	120.61	121.97
CN, NH_2[d]	1.4086	1.3376	1.4379	1.4141	1.0788	1.0812	178.29	107.58	113.54	103.84	102.79	120.60	121.98
F, H	1.3523	1.3588	1.3514	1.0806	1.0805	1.0800	185.86	106.83	105.99	106.89	105.04	118.86	120.21
NH_2, OH	1.3360	1.3990	1.4271	1.3857	1.0817	1.0852	174.45	113.83	103.32	103.66	105.60	122.02	120.29
Cl, H	1.3539	1.3474	1.7610	1.0801	1.0769	1.0797	178.82	107.87	105.72	106.42	104.81	119.01	120.20
OH, Cl	1.3371	1.3574	1.3822	1.7632	1.0841	1.0764	185.53	103.84	107.73	104.68	106.10	120.51	119.04
CN, OH[e]	1.3859	1.3467	1.4394	1.3670			165.98	103.80	107.61				
CN, OH[d]	1.3506	1.3553	1.4410	1.3785	1.0785	1.0835	171.28	107.85	103.12	103.66	104.22	120.77	120.41
OH, F	1.3503	1.3575	1.3845	1.3524	1.0843	1.0800	184.37	103.46	107.62	105.18	106.24	120.38	119.09
NH_2, Cl	1.3207	1.4149	1.4214	1.7635	1.0817	1.0771	179.28	113.81	107.45	103.41	106.62	122.01	118.82
OH, H	1.3471	1.3595	1.3843	1.0807	1.0798	1.0849	185.69	106.07	104.31	104.92	105.17	120.26	120.54
NH_2, F	1.3354	1.4077	1.4251	1.3541	1.0819	1.0809	174.21	114.09	105.94	103.58	107.42	122.06	118.55
CN, Cl	1.3424	1.3626	1.4413	1.7527	1.0788	1.0765	177.57	107.49	107.23	103.75	105.26	120.66	119.15
CN, F	1.3500	1.3625	1.4411	1.3446	1.0788	1.0792	171.70	107.72	105.63	103.87	105.98	120.71	118.66
NH_2, H	1.3316	1.4091	1.4272	1.0804	1.0823	1.0807	177.38	113.16	105.64	104.29	105.43	121.80	120.02
CN, H	1.3478	1.3649	1.4424	1.0795	1.0789	1.0792	180.40	107.65	105.09	104.40	104.33	120.54	120.17

[a] The geometrical parameters are defined in Figure 1. [b] Bond lengths in angstroms and angles in degrees. [c] For the C_1 symmetry structures the average of the geometrical parameters are given. [d] C_s symmetry structure. [e] The complete structure of this transition state is given in Figure 3.

hydrogen bond and the formation of the product carbon–hydrogen bond. Total atomic charges were obtained from a Mulliken population analysis at the UHF/6-31G** level.

Discussion

The total energies, zero point vibrational energies, and S^2 values are collected in Table I; optimized geometries of the transition states are summarized in Figure 1 and Table II. All data are tabulated with the symmetric reactions listed first followed by the cross reactions in the order of increasing exothermicity (as calculated at the HF/6-31G** level); all discussions will pertain to the reactions progressing in the exothermic direction. The symmetric transition states (X = Y) were obtained by optimizations constrained to C_{2h} symmetry, except for X = H, which is of D_{3d} symmetry. Other rotamers of the transition states may exist but are expected to be of very similar energy. All of the symmetric transition states have the odd electron in the anti-

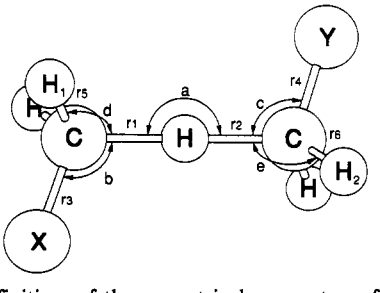

Figure 1. Definitions of the geometrical parameters of the transition states. The dihedral angles Ω_1 and Ω_2 are defined as the angles of H_1 and H_2 to the X–C–H–C–Y plane.

symmetric combination of the σ bonds being formed and broken (this corresponds to the ^2B_u electronic state in the C_{2h} point group and the $^2A_{2u}$ state[10] in the D_{3d} point group). Comparison of the

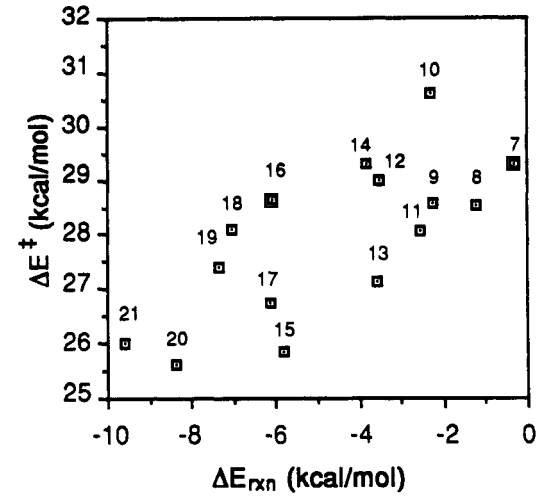

a

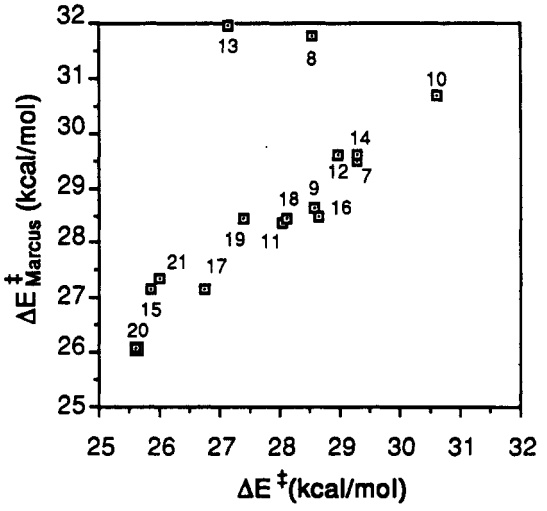

b

Figure 2. (a) Plot of the UHF/6-31G** barrier height of the reactions versus the change in energy of reaction (the numbers correspond to the reaction numbers listed in Table III). (b) Plot of the barrier heights predicted by Marcus theory versus the UHF/6-31G** barrier heights.

geometries of the different symmetric transition states shows that the carbon–hydrogen bonds being formed/broken are all 1.36 ± 0.02 Å. The symmetric transition states have barriers ranging from 29 to 35 kcal/mol. The imaginary frequencies that correspond to the reaction coordinate are in the range of 2500*i*–2700*i* wavenumbers. The lowest energy molecular vibrations have frequencies of approximately 20 wavenumbers for the internal rotation mode, indicating the surface is very flat in the region of the transition state.

For each of the 15 cases, the electronic structure of the cross transition state (X ≠ Y) is characterized by the odd electron in an orbital corresponding to the out of phase combination of the σ orbitals for the bonds being formed/broken. All of the cross transition states except X = CN and Y = NH_2 or OH are of C_s point group symmetry. For the X = CN and Y = NH_2 or OH, the C_s structures are a maximum with respect to two degrees of freedom; further optimization leads to C_1 symmetry transition structures with a single imaginary frequency. The X = CN and Y = NH_2 transition state breaks the planar symmetry by only 0.1°; however, the X = CN and Y = OH transition state adopts a conformation with the OH and CN groups gauche. Details of

(10) At the UHF/3-21G level the X = Y = H transition state is in the $^2A_{2u}$ state and at the UHF/6-31G** level the wave function has broken symmetry (lower symmetry than the nuclear framework).

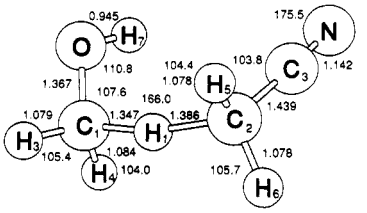

Figure 3. UHF/6-31G** structure of X = CN and Y = OH transition state. Bond lengths are in angstroms and angles in degrees. The dihedral angles in degrees are $O–C_1–H_1–C_2$ = 19.1, $C_1–H_1–C_2–C_3$ = 24.4, $H_1–C_2–C_3–N$ = 2.9, $H_3–C_1–H_1–C_2$ = 136.9, $H_4–C_1–H_1–C_2$ = −103.7, $H_5–C_2–H_1–C_1$ = −95.1, $H_6–C_2–H_1–C_1$ = 144.4, $H_7–O–C_1–H_1$ = −67.8.

the geometry of the $HOCH_2–H–CH_2CN$ transition state are given in Figure 3. Inspection of the geometries of the cross transition states, listed in Table II and depicted in Figure 1, shows that these reactions do not follow Hammond's postulate rigorously; however, there is a general tendency for the breaking carbon–hydrogen bond to be shorter than the forming bond when the reaction proceeds in the exothermic direction. The variation in the forming/breaking carbon–hydrogen bonds is slightly higher than the symmetric reactions (R(C–H) = 1.36 ± 0.05 Å). The changes in the bond lengths are so small that no useful trends can be extracted. The range of the UHF/6-31G** barrier heights for the cross reactions is 25–31 kcal/mol. The imaginary frequencies that correspond to the reaction coordinate are between 2400*i* and 2700*i* wavenumbers. These transition states also have a very low frequency molecular vibration (2–32 wavenumbers) corresponding to a very flat potential energy surface with respect to internal rotation in the transition state.

The UHF/3-21G, UHF/6-31G**, and the Marcus barrier heights are reported in Table III. As can be seen in Figure 2a there is a slight trend for the reaction barrier to decrease as the exothermicity increases; however, the scatter in the data prevents this trend from being useful in predicting the barrier heights. By contrast Figure 2b shows that the agreement between the Marcus barrier heights and the ab initio barrier heights is very good, except for the cases of X = CN and Y = NH_2 or OH. Even in these cases the errors are only 3.23 and 4.82 kcal/mol too high. The average error for the Marcus barriers is 1.42 kcal/mol at the HF/3-21G level, 0.98 kcal/mol at the HF/6-31G** level using all of the data, and 0.52 kcal/mol if the points for X = CN and Y = NH_2 or OH are ommitted. At least-squares fit of a straight line to the data in Figure 2b yields a correlation coefficient of 0.85.

There are two factors that contribute to the difference between Marcus theory and ab initio barrier heights: changes in geometry and changes in electronic structure. The largest errors are for the transition states that break the planar symmetry, X = CN and Y = OH or NH_2. Both of these planar structures are second-order saddle points (each has two imaginary frequencies) that are 3.03 and 0.0002 kcal/mol higher in energy than the real transition states. This explains most of the discrepancy for the X = CN, Y = OH transition state; however, the origin of the forces that cause the change in geometry require further investigation.

An understanding of the electronic structure factors that influence the barriers can be obtained from state correlation diagrams and the curve-crossing model. These approaches have been used quite effectively to analyze and interpret barrier heights for a variety of chemical reactions.[11,12] Shaik[13] has pointed out that the electronic structure of transition states can include significantly greater contributions from higher lying electronic states than the reactants or products. Near the transition state the energy surfaces

(11) (a) Maitre, P.; Hiberty, P. C.; Ohanessian, G.; Shaik, S. S. *J. Phys. Chem.* **1990**, *94*, 4089. (b) Sini, G.; Ohanessian, G.; Hiberty, P. C.; Shaik, S. S. *J. Am. Chem. Soc.* **1990**, *112*, 1407. (c) Shaik, S. S.; Canadel, E. *J. Am. Chem. Soc.* **1990**, *112*, 1446.

(12) Pross, A.; Yamataka, H.; Nagase, S. *J. Phys. Org. Chem.* **1991**, *4*, 135.

(13) Shaik, S. S.; Schlegel, H. B.; Wolfe, S. *Theoretical Aspects of Physical Organic Chemistry. The S_N2 Mechanism*; Wiley: New York, in press.

TABLE III: Changes in Energy of Reaction ab Initio Barrier Heights, Marcus Predicted Barrier Heights (All in kcal/mol), and Group Charge Differences

		UHF/3-21G				UHF/6-31G**				
	X, Y	ΔE_{rxn}	$\Delta E^{\ddagger}$	$\Delta E^{\ddagger}_{Marcus}$	error	ΔE_{rxn}	$\Delta E^{\ddagger}$	$\Delta E^{\ddagger}_{Marcus}$	error	$q_x - q_y$[a]
1	H, H		27.20				29.73			
2	F, F		28.15				29.77			
3	Cl, Cl		25.18				29.50			
4	OH, OH		42.02				33.16			
5	NH_2, NH_2		28.46				30.50			
6	CN, CN		30.91				34.26			
7	Cl, F	4.84	28.73	29.14	0.41	−0.30	29.28	29.49	0.21	−0.083
8	CN, NH_2[b]	−1.48	25.47	28.95	3.48	−1.25	28.53	31.76	3.23	−0.235
	CN, NH_2[c]	−1.48	25.47	28.95	3.48	−1.25	28.53	31.76	3.23	−0.235
9	F, H	−3.14	26.04	26.12	0.08	−2.25	28.57	28.64	0.07	−0.002
10	NH_2, OH	7.87	36.52	39.28	2.76	−2.30	30.60	30.69	0.09	0.089
11	Cl, H	1.70	26.42	27.05	0.63	−2.55	28.04	28.36	0.32	−0.084
12	OH, Cl	−19.39	23.02	24.60	1.58	−3.51	28.98	29.60	0.62	0.072
13	CN, OH[b]	6.39	35.93	39.72	3.79	−3.55	27.14	31.96	4.82	−0.201
	CN, OH[c]	6.39	38.22	39.72	1.50	−3.55	30.17	31.96	1.79	−0.127
14	OH, F	−14.55	27.34	28.18	0.84	−3.81	29.29	29.59	0.30	−0.017
15	NH_2, Cl	−11.53	18.83	21.37	2.54	−5.81	25.84	27.17	1.33	0.166
16	OH, H	−17.69	26.19	26.33	0.14	−6.06	28.65	28.49	−0.16	−0.012
17	NH_2, F	−6.68	22.50	25.06	2.56	−6.11	26.74	27.16	0.42	0.082
18	CN, Cl	−13.01	21.77	21.92	0.15	−7.06	28.10	28.44	0.34	−0.059
19	CN, F	−8.16	24.96	25.59	0.63	−7.36	27.38	28.44	1.06	−0.135
20	NH_2, H	−9.83	22.57	23.13	0.56	−8.36	25.62	26.08	0.46	0.075
21	CN, H	−11.31	22.53	23.68	1.15	−9.61	25.99	27.37	1.38	−0.141

[a] The charges, $q_{x(y)}$ are defined as the sum of the Mulliken total atomic charges of the $CH_2X(Y)$ moieties. [b] C_1 symmetry structure. [c] C_s symmetry structure.

TABLE IV: UHF/6-31G Vibrational Frequencies in Wavenumbers for the Transition States**

X, Y	ν_i	all other vibrational frequencies[a]
H, H	2531*i*	41, 346 (2), 504, 760 (2), 1271, 1289, 1469 (2), 1569 (2), 1589 (2), 3210, 3212, 3338, 3338, 3339 (2)
F, F	2637*i*	23, 70, 204, 328, 556, 747, 1201, 1212, 1282, 1305, 1312, 1350, 1539, 1540, 1612, 1628, 3245, 3245, 3343, 3345
Cl, Cl	2635*i*	16, 83, 155, 337, 548, 730, 810, 824, 1129, 1157, 1157, 1237, 1514, 1534, 1552, 1552, 3248, 3284, 3390, 3391
OH, OH	2621*i*	23, 85, 132, 141, 218, 353, 552, 766, 1165, 1194, 1208, 1225, 1281, 1288, 1400, 1414, 1529, 1569, 1631, 1637, 3194, 3194, 3272, 3276, 4157, 4157
NH_2, NH_2	2603*i*	24, 91, 212, 215, 301, 430, 504, 714, 871, 914, 1049, 1093, 1171, 1198, 1238, 1297, 1469, 1469, 1563, 1568, 1594, 1606, 1805, 1806, 3218, 3218, 3292, 3294, 3754, 3847, 3847
CN, CN	2697*i*	15, 69, 142, 341, 408, 409, 427, 460, 609, 766, 1017, 1026, 1129, 1163, 1167, 1191, 1465, 1495, 1567, 1569, 2409, 2415, 3277, 3277, 3364, 3364
Cl, F	2622*i*	24, 78, 181, 335, 555, 738, 809, 1146, 1182, 1225, 1308, 1323, 1529, 1545, 1552, 1623, 3247, 3283, 3348, 3389
CN, NH_2	2431*i*	9, 77, 189, 264, 406, 431, 452, 570, 744, 810, 1025, 1065, 1120, 1191, 1224, 1268, 1459, 1524, 1543, 1571, 1602, 1808, 2429, 3420, 3269, 3322, 3352, 3777, 3878
F, H	2576*i*	32, 119, 338, 503, 625, 755, 1210, 1281, 1311, 1313, 1503, 1512, 1580, 1583, 1624, 3213, 3238, 3334, 3340, 3346
NH_2, OH	2563*i*	2, 91, 162, 217, 260, 414, 528, 737, 876, 1067, 1161, 1202, 1208, 1283, 1288, 1396, 1465, 1549, 1571, 1602, 1632, 1806, 3181, 3234, 3258, 3310, 3760, 3854, 4154
Cl, H	2566*i*	31, 119, 341, 485, 613, 745, 817, 1150, 1202, 1287, 1488, 1496, 1554, 1576, 1580, 3216, 3279, 3346, 3351, 3383
OH, Cl	2609*i*	22, 86, 95, 187, 341, 551, 745, 807, 1143, 1166, 1205, 1231, 1284, 1411, 1521, 1550, 1559, 1635, 3198, 3280, 3285, 3392, 4157
CN, OH	2483*i*	65, 82, 189, 362, 411, 445, 523, 566, 721, 1019, 1117, 1181, 1192, 1248, 1307, 1486, 1517, 1542, 1569, 1625, 2441, 3214, 3277, 3331, 3364, 4167
OH, F	2628*i*	26, 80, 135, 212, 340, 554, 756, 1176, 1207, 1214, 1284, 1308, 1319, 1409, 1534, 1553, 1619, 1635, 3195, 3244, 3275, 3343, 4157
NH_2, Cl	2488*i*	10, 85, 191, 257, 417, 523, 717, 805, 846, 1064, 1154, 1159, 1217, 1284, 1463, 1543, 1550, 1558, 1602, 1808, 3235, 3274, 3313, 3379, 3768, 3865
OH, H	2572*i*	17, 135, 143, 351, 502, 622, 764, 1189, 1213, 1274, 1288, 1411, 1498, 1518, 1578, 1588, 1635, 3187, 3213, 3264, 3339, 3347, 4159
NH_2, F	2559*i*	14, 78, 210, 253, 406, 530, 725, 861, 1069, 1186, 1205, 1256, 1311, 1322, 1465, 1553, 1561, 1598, 1621, 1807, 3231, 3232, 3308, 3328, 3764, 3859
CN, Cl	2645*i*	18, 76, 152, 339, 421, 435, 584, 749, 825, 1018, 1135, 1136, 1185, 1208, 1489, 1515, 1551, 1569, 2435, 3273, 3285, 3358, 3395
CN, F	2602*i*	23, 72, 172, 336, 422, 448, 591, 759, 1020, 1152, 1183, 1228, 1306, 1307, 1505, 1536, 1570, 1622, 2435, 3245, 3273, 3356, 3360
NH_2, H	2508*i*	32, 138, 248, 409, 472, 600, 732, 896, 1070, 1198, 1248, 1274, 1467, 1523, 1523, 1581, 1582, 1602, 1807, 3207, 3226, 3301, 3333, 3336, 3758, 3851
CN, H	2549*i*	19, 106, 340, 425, 432, 478, 660, 763, 1020, 1154, 1187, 1281, 1470, 1480, 1568, 1568, 1573, 2451, 3220, 3270, 3353, 3356, 3360

[a] Degeneracies are noted in parentheses.

representing the ground-state and excited-state valence bond configurations are closer together than at the reactants or products. Hence, these configurations can interact more strongly. The net effect on the ground-state surface is a lowering of the barrier, as shown in Figure 4. Pross et al.[12] have computed the transition states and barrier heights for a series of hydrogen abstraction reactions RH + $^{\bullet}X \rightarrow R^{\bullet} + HX$ (R = Me, Et, iPr, tBu; X = H, Cl, R). In analyzing those barriers using the curve-crossing model, they found significant charge-transfer contributions for RH + Cl.

An estimate of the contribution of ionic configurations can be obtained from the charge distribution in the transition state. Group charges, q_x and q_y, have been calculated as the sum of the Mulliken total atomic charges for the CH_2X and CH_2Y groups. Charge differences, $q_x - q_y$, are listed in Table III. Half of the absolute value of the charge differences, $|q_x - q_y|/2$, translates directly into the weight of the ionic configuration, ω_{ct}, of the transition states.

$$X^{q_x}CH_2\text{-}H\text{-}CH_2Y^{q_y} = \omega_{cov}XCH_2\text{-}H\text{-}CH_2Y + \omega_{ct}X^{+1}CH_2\text{-}H\text{-}CH_2Y^{-1} \quad q_x = \omega_{ct};\ q_y = -\omega_{ct}$$

$$X^{q_x}CH_2\text{-}H\text{-}CH_2Y^{q_y} = \omega_{cov}XCH_2\text{-}H\text{-}CH_2Y + \omega_{ct}X^{-1}CH_2\text{-}H\text{-}CH_2Y^{+1} \quad q_x = -\omega_{ct};\ q_y = \omega_{ct}$$

$$|\omega_{ct}| = \frac{|q_x - q_y|}{2}$$

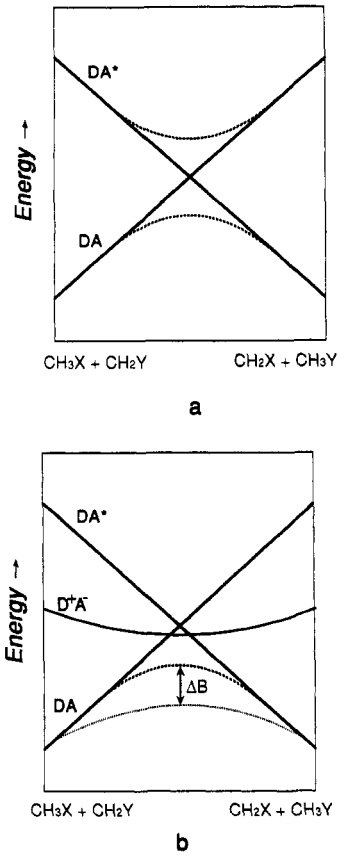

Figure 4. State-correlation diagrams for the radical abstraction reactions; D = donor, A = acceptor, the solid lines are the diabatic representation, and the dashed lines are the adiabatic representation with (a) no excited-state interaction. (b) a low-lying excited state interacting with the ground state; long dashed line is the unperturbed ground state, the short dashed line is the ground state perturbed by the presence of a low-lying excited state. This interaction has lowered the barrier on the ground-state surface by ΔB.

All five reactions that have an error exceeding 0.7 kcal/mol have a charge difference exceeding 0.10 electron in absolute value and the two largest errors correspond to the two largest charge differences. Figure 5 shows the correlation between the contribution of charge transfer and the error between the Marcus theory and ab initio barrier heights. To separate the effects of structural changes and charge transfer on the energy of the transition states, the C_s symmetry structures have been used throughout.[14] A

(14) The C_s and C_1 symmetry structures with X = CN and Y = NH_2 have the same error and charge differences; however the error and charge difference for the X = CN and Y = OH C_s structure are 1.79 kcal/mol and −0.127 electron versus the C_1 values of 4.82 kcal/mol and −0.201 electron.

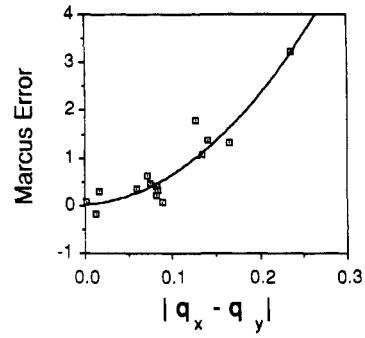

Figure 5. Plot of the error in the Marcus predicted barrier heights versus the charge differences.

least-squares fit of a quadratic polynomial to the data in Figure 5 gives a correlation coefficient of 0.94.

The above results provide direct evidence that ionic states can play a larger role in the electronic structure of the transition states for the cross reactions than in the symmetric transition states. For the series of radical abstraction reactions studied, charge-transfer states can be major contributors to the electronic structure of the transition states. These charge-transfer states can be represented as resonance structures of the form

$$AH_2C\cdots H\cdots CH_2D \leftrightarrow A^-H_2C\cdots H\cdots CH_2D^+ \qquad (3)$$

where D is an electron-donor group and A is an electron-withdrawing group. This effect has also been termed captodative or push–pull stabilization.

Conclusion

Marcus theory accurately predicts the barriers for all of the reactions $CH_3X + {}^{\bullet}CH_2Y \rightarrow {}^{\bullet}CH_2X + CH_3Y$ (X, Y = H, F, Cl, OH, NH_2, CN) except X = CN and Y = NH_2 or OH. Charge-transfer states have been found to be a major contributor to the electronic structure of these two transition states and a minor contributor for a few others. The agreement for the vast majority of the Marcus barrier heights should extend to higher levels of theory (larger basis sets and inclusion of electron correlation).

Acknowledgment. We would like to thank the National Science Foundation for financial support (Grant No. CHE 90-20398) and the Pittsburgh Supercomputing Center for a grant of computer time.

Registry No. H, 1333-74-0; CH_3F, 593-53-3; CH_3Cl, 74-87-3; CH_3OH, 67-56-1; CH_3NH_2, 74-89-5; CH_3CN, 75-05-8; CH_3H, 74-82-8; CH_3, 2229-07-4; CH_2F, 3744-29-4; CH_2Cl, 6806-86-6; CH_2OH, 2597-43-5; CH_2NH_2, 10507-29-6; CH_2CN, 2932-82-3.